arXiv:astro-ph/0110550v1 25 Oct 2001

An Adaptive Optics Search for Companions to Stars with Planets

K. L. Luhman

Harvard-Smithsonian Center for Astrophysics, 60 Garden St., Cambridge, MA 02138

kluhman@cfa.harvard.edu

and

Ray Jayawardhana

Department of Astronomy, University of California, 601 Campbell Hall, Berkeley, CA 94720

rayjay@astro.berkeley.edu

ABSTRACT

We have performed a Keck adaptive optics (AO) imaging survey of 25 extrasolar planetary systems discovered by the radial velocity programs. Typically, the high-resolution (FWHM$\sim$ $0\farcs04$) near-infrared images are able to detect point sources at $\Delta H = 10$ at $1''$, L and T dwarfs at $0\farcs5$ to $2''$, and stars and brown dwarfs at 3-10 AU and 10-100 AU from the targets. The AO images reveal 15 faint sources (H = 14-20) near the stars HD 37124, HD 168443, HD 187123, and HD 190228 out to a search radius of $3\farcs3$. We have obtained AO images at a second epoch for five of the candidate companions at Keck and Gemini Observatories. The resulting measurements of proper motions relative to the primary stars indicate that these five sources are background stars. Given that the four primaries are near the Galactic plane ($|b| < 6°$), the remaining faint sources are also likely to be background stars rather than substellar companions. We present the companion detection limits for each target as a function of separation and compare them to the sensitivities of radial velocity surveys, demonstrating the complementary nature of the two techniques.

Subject headings: planetary systems – techniques: high angular resolution – binaries: close – stars: low-mass, brown dwarfs

1. Introduction

In the search for planetary companions outside of our solar system, a variety of techniques have been devised and implemented, of which radial velocity monitoring has proven the most successful to date. Such measurements have led to the discovery of planets with masses of $> 0.3\ M_{\rm Jup}$ and separations of a few AU or less around ~ 60 nearby stars (Mayor & Queloz 1995; Marcy & Butler 1996; Cochran et al. 1997; Noyes et al. 1997; Udry, Mayor, & Queloz 2001; Butler et al. 2000; Fischer et al. 2001b; Tinney et al. 2001). Combining those results with data on spectroscopic binaries produces a distribution of companions from 1-1000 $M_{\rm Jup}$ that is characterized by a minimum or "brown dwarf desert" at 10-30 $M_{\rm Jup}$ (e.g., Marcy & Butler 1998). This feature is likely a reflection of two formation mechanisms, one that creates planets from disks and one that produces companion stars and brown dwarfs (e.g., core fragmentation). However, to fully understand the processes of planet and binary star formation, it is essential that the frequency of companions

is measured over the maximum possible range of separations. For instance, the conspicuous paucity of brown dwarf companions at $\lesssim 5$ AU may not exist at separations beyond 1000 AU (Gizis et al. 2001).

Known extrasolar planetary systems are logical initial targets for a search for companions at modestly wide separations (10-100 AU). Gravitational perturbations by outer substellar or stellar companions may be responsible for the eccentric orbits observed for many planetary companions. To properly evaluate the stability and evolution of these planets (e.g., Rivera & Lissauer 2000), wide massive companions must be searched for and included in the analysis. Furthermore, if substellar companions can be resolved from primaries, spectroscopic analysis would provide constraints on masses, temperatures, surface gravities, and compositions, and thus contribute to our understanding of the physical characteristics of substellar objects (Marley et al. 1996; Allard et al. 1996). Finally, as radial velocity measurements are accumulated over longer periods of time, they are becoming sensitive to companions at larger separations. It already appears that at least 50% of stars with planets have additional distant companions (Marcy et al. 2001a, b; Fischer et al. 2001b), which suggests that a search for a substellar objects at still wider separations through high-resolution direct imaging could prove fruitful.

Direct imaging has become increasingly effective in detecting faint companions to bright stars. In high-resolution imaging with WFPC2 aboard the *Hubble Space Telescope (HST)*, Schroeder et al. (2000) probed for massive and young brown dwarfs at 1-60 AU from 23 nearby stars. From the ground, Oppenheimer et al. (2001) used optical coronographic data and near-infrared (IR) images to search for companions at 40-120 AU and > 40 $M_{\rm Jup}$ near most of the known stars within 8 pc, which resulted in the discovery of the brown dwarf companion Gl 229B (Nakajima et al. 1995). The tip-tilt techniques used for enhanced image quality by Oppenheimer et al. (2001) have been followed by higher order adaptive optics (AO) systems that achieve comparable and sometimes superior spatial resolution and sensitivity to those of HST. Near-IR AO imaging already has been used to discover binary systems whose members are near the hydrogen burning mass limit (Martín et al. 2000; Close et al. 2002). In addition, AO has been performed in conjunction with radial velocity measurements of nearby stars (Delfosse et al. 1999) and has resulted in the discovery of a brown dwarf companion (~ 50 $M_{\rm Jup}$, $H = 14.4$) to the planet-bearing star Gl 86 (Els et al. 2001). In this paper, we present the results of a survey for companions to 25 planetary systems using near-IR AO imaging at Keck Observatory. We report astrometry and photometry for several point sources found in these images and discuss their likely origin as companions or background field stars. We characterize the detection limits of these data in both observational and physical units, which are then compared to the sensitivities of the radial velocity surveys, and we discuss the implications of these data for individual planet-bearing stars.

2. Observations and Data Analysis

2.1. Adaptive Optics Imaging

During the nights of 2000 May 10, June 27, and September 16-18, we used the Shack-Hartmann AO system on the Keck II telescope (Wizinowich et al. 2000) in conjunction with KCam, a NICMOS3 256×256 near-IR camera, to obtain images of 25 stars for which planetary companions have been discovered in previous radial velocity measurements. Properties of the planetary systems in our sample are given in Table 1. The plate scale of KCam was $0\farcs01744 \pm 0\farcs0005$ pixel^{-1}, corresponding to a total field of $4\farcs46 \times 4\farcs46$. The lower right quadrant of the array was not functional. A cold filter wheel contained J, H, and K' filters. Warm external filters included an open filter and neutral density filters that attenuated the signal by factors of 10, 100, and 1000 (N1, N2, and N3). The H-band filter was selected for all observations because it produces

the optimum combination of spatial resolution and sensitivity and because substellar objects are relatively bright in this band.

The targets were grouped into pairs of stars that were close together on the sky ($\lesssim 15°$). The stars in a pair were observed in succession so that the data for one star provided an estimate of the PSF for the other star. Images for a given star were obtained in the following manner. The star was first centered in one of the three operating quadrants of the array. The exposure time and neutral density filter were selected such that the maximum number of counts in the image was between 50 and 80% of the saturation level, where 5 sec and N3 were typical choices for a star at $H = 5$. Multiple exposures were obtained at each of two positions that were separated by $0\farcs0872$ (5 pixels) along the rows and columns of the array. Similar exposures were obtained through the less opaque neutral density filters and the open filter to reach successively fainter magnitudes. The same steps were then followed for the star that was paired to this target. These data are used to search for companions within the quadrant surrounding each star ($< 1\farcs1$). The following observations were designed to reach larger separations. A target was centered in the upper left quadrant of the camera array. Because the area of the array directly surrounding the target was already imaged and would be saturated in long exposures, the telescope was offset by $2\farcs232$ (128 pixels) in each direction on the array to place the star near the center of the lower right dead quadrant. Three images were obtained at each position in the same dither pattern used previously. Each image consisted of the sum of two exposures with integration times of 30 sec for most stars and 5 sec for the brightest targets, which were short enough to avoid saturation within the operating quadrants of the array. As a result, the total integration time was typically 6 min. These steps for the long exposures were repeated at two additional position angles at intervals of 120°, providing full and partial coverage out to radii of $3\farcs3$ and $4\farcs6$ surrounding each star. The position angle of the array was fixed during a given image.

We now comment on a few departures from the above observing strategy. The observations of ρ^1 55 Cnc and 47 UMa differed from the standard procedure because the observations of these two objects were completed before the final strategy was adopted. Only the N3 and open external filters were used for these stars. In addition, only short exposure times were used for 47 UMa. Similarly, only short exposures were obtained for HD 168443 on the first night of observations. As a result, only the brightest two objects near HD 168443 in Table 2 were detected in those data. A complete data set with the final observing procedure was obtained for HD 168443 during the later observing runs. The faint objects near the HD187123, HD37124, and HD168443 were noticed in the data that were reduced at the telescope. To facilitate the measurement of the positions of these sources relative to the primaries, we obtained additional exposures in which both the faint sources and the primaries appeared in good quadrants of the array.

Two of the stars with faint nearby sources in the Keck data, HD 187123 and HD 37124, were observed with the University of Hawaii Hokupa'a AO system in conjunction with the 1024×1024 near-IR camera QUIRC (Graves et al. 1998) on the Gemini North telescope during the night of 2001 October 7. The plate scale of QUIRC was $0\farcs01998 \pm 0\farcs0008$ pixel^{-1}, corresponding to a total field of $20\farcs46 \times 20\farcs46$. We obtained twelve 30 sec exposures of HD 187123 and seven 1 sec exposures of HD 37124 through the H-band filter. These exposure times were selected to minimize the saturation of the primary stars while providing sufficient sensitivity to detect the faint sources found in the Keck data, thus optimizing the astrometry for those sources relative to the primaries. The Gemini AO data for HD 187123 and HD 37124 exhibited FWHM= $0\farcs14$ and $0\farcs09$, respectively.

2.2. Image Processing

Standard data reduction procedures were followed for the AO images. The Keck images were divided by twilight sky flat frames, while the Gemini data were divided by dome flat frames. Offsets between dithered frames were measured from the centroids of nonsaturated point sources or the isophotes around saturated stars. Dithered frames were then combined into one image.

The properties of the Keck AO data are illustrated in Figure 1, which shows images of 51 Peg at various signal levels. The AO-corrected PSF is characterized by a bright narrow core whose width (FWHM$\sim 0\farcs04 =$ 2.3 pixels) approaches the diffraction limit and a low-level broad halo that is comparable in size to the seeing disc (FWHM$\sim 0\farcs5 = 29$ pixels). Astronomical point sources must be distinguished from point-like speckles that reside within the halo. This was accomplished by visually comparing the images of a given pair of targets that were observed consecutively and thus act as PSF stars for each other. In addition, because most of the PSF features rotate on the array (and thus the sky) with time, we could distinguish speckles from astronomical sources by comparing the images at the individual dither positions for a star. At larger radii from a star, the features of the PSF are radially elongated and therefore are not mistaken for companions. The sources that were found in this manner are listed in Table 2. Images of the objects detected near HD 37124, HD 168443, HD 187123, and HD 190228 are shown in in Figs. 2-6.

The array coordinates and photometry of the point sources near the target stars were measured with the IRAF tasks IMEXAMINE and PHOT, respectively. Aperture photometry was extracted with a radius of 3 to 6 pixels in the Keck data, where fainter sources were measured with smaller radii. Photometric calibration was derived from aperture photometry with radii of 40 pixels of the unsaturated images of the target stars. When available, the H-band measurements from the Two-Micron All-Sky Survey were adopted. Otherwise, the H magnitudes were estimated by combining the spectral types and visual magnitudes of the targets. Most of the Keck images were obtained in photometric conditions and the calibrations implied by the various targets agree within ± 0.1 mag. Because the conditions were not photometric during the Gemini observations, photometry is not measured from those data. After measuring the aperture corrections between 40 and 3-6 pixels from the unsaturated Keck images of the targets, we arrived at H-band magnitudes for the point sources, which are given in Table 2. Because the fraction of the star's light that falls within the PSF core can change significantly between consecutive images, the absolute photometry has large uncertainties of $\sim \pm 0.5$ mag. Multiple observations of the point source near HD 37124 suggest a smaller photometric error of $\sim \pm 0.2$ mag. Because the two sources near HD 187123 were measured in the same image, their relative photometry should have good precision ($\sim \pm 0.1$ mag). Similarly, the relative positions of multiple sources near a star have small errors (± 0.25 pixels). Meanwhile, the offsets of the faint sources from the central stars are more uncertain because the latter were saturated or in the dead quadrant in the images where the former were detected. As described in the previous section, extra images were obtained for HD 37124, HD 187123, and HD 168443 so that the faint sources and the primaries would both appear in good quadrants of the array. The uncertainties in the offsets between saturated primaries and the surrounding objects are ± 1 pixel in each direction on the array. In the Gemini data, both the candidate companions and the primaries fell within the array as well. For the faint sources near HD 190228, we have only the original long exposures in which the primary fell in the dead quadrant. In these data, we used the isophotes of the primary's PSF that extended into the good quadrants to estimate the position of the primary, and thus the offset between the faint sources and the primary. The uncertainties in those offsets are ± 2 pixels. By obtaining images of an artificial light source within the Keck AO system at several positions across the array, we measured a plate scale of $0\farcs01744$ pixel^{-1} for KCam. A plate scale of $0\farcs01998$ pixel^{-1} in the H-band has been measured for the QUIRC camera on Gemini by F. Rigaut. These plate scales were combined with the position angles of

the instruments and the pixel offsets to compute the offsets in right ascension and declination that are listed in Table 2.

2.3. Measurement of Detection Limits

We now characterize the sensitivity to companions of the Keck AO data. We began by measuring the H-band detection limits for point sources as a function of angular separation from the targets. To remove the large-scale shape of the PSF of the target stars, each image was convolved with a two-dimensional Gaussian function and divided into the original image. In the quotient image, we measured the standard deviation in five pixel square boxes at one pixel intervals along a line radially outward from star, which was then repeated for radial lines at several other angles around the star that avoided ghost images of the primary. At the image positions measured in this way, we inserted artificial stars that simulated the core of the PSF, which were given the FWHM measured from the unsaturated image of the star and a peak intensity that equaled a multiple of the standard deviation measured at that point in the image. After visually examining the artificial stars at several values of this multiple, we adopted six sigma as a reasonable representation of the detection limit. The sources detected around HD 190228 in Figure 6 are near this detection limit. In addition, eight artificial stars have been placed at the detection limit of $\Delta H = 10$ at $1''$ in one of the images of 51 Peg in Figure 1. Within the seeing disc, the presence of speckles complicates the characterization of the detection limit. As discussed in the previous section, real point sources can be identified down to the amplitude of the speckles. As a result, the speckles effectively define the detection limit for point sources. Because the six sigma deviations measured from 5 pixel boxes in the seeing disc were comparable to the speckles intensities (i.e., the speckles are sparsely distributed relative to this box size), we adopted the former measurement for characterizing the detection limit both inside and outside of the seeing disc. For a given star, the H-band detection limits were measured for the various filters, exposure times, and position angles and the combined results were fit by one polynomial function. The differences of the H-band detection limits for point sources and the magnitudes of the target stars (ΔH) are presented as a function of angular separation in Figs. 7-13. The ghost images that appear in the long exposures result in an 2-3% incompleteness in areal coverage. Because the observations of ρ^1 55 Cnc and 47 UMa were not optimized for dynamic range, the images were less sensitive to companions at intermediate separations, as indicated by the data for these stars in Figure 9. In addition, the detection limit at large separations for 47 UMa was worse than for the other stars because only short exposures were obtained.

As an illustration of the sensitivity to companions of these data, in Figs. 7-13 we have indicated the magnitudes of typical L and T dwarfs at the distances of the targets. We considered all field dwarfs between spectral types of M9 V and T that have trigonometric parallaxes as compiled by Kirkpatrick et al. (2000). For these objects, we fit a polynomial function to spectral type versus M_H for M9 V through L8 V, where the data were from Kirkpatrick et al. (2000) and references therein. The values of M_H from this function for L0 V, L5 V, and L8 V and the measurements of M_H for the T dwarfs Gl 229B and Gl 570D (Kirkpatrick et al. 2000; Leggett et al. 1999) are plotted along the detection limits of separation versus ΔH in Figs. 7-13.

The H-band detection limits for companions have been transformed to units of mass and projected physical separation in the following manner. Conversions between spectral types and effective temperatures are from Schmidt-Kaler (1982) for $\leq$M0 V and from Leggett et al. (1996) as presented by Luhman (1999) for M1 V to M9 V. For L and T types, we adopted a conversion in which L0 V, L8 V, and the T dwarf Gl 229B correspond to effective temperatures of 2000, 1400, and 900 K (Leggett et al. 1999, 2001; Kirkpatrick et al. 2000; Reid et al. 2001b; Schweitzer et al. 2001). Bolometric corrections are from Kenyon & Hartmann (1995)

for <M6 and from Bessell (1991), Monet et al. (1992), Tinney, Mould, & Reid (1993), and Leggett et al. (1996) for M6 to M9. For L and T types, the H-band bolometric corrections were computed from the J-band corrections of Reid et al. (2001a) and the average $J - H$ colors of Kirkpatrick et al. (2000). By combining these conversions with the H-band magnitudes and angular separations of the detection limits, the distances of the targets, and theoretical mass-luminosity relations for 1, 3, and 10 Gyr ($\geq 0.1\ M_{\odot}$, Baraffe at al. 1998; $< 0.1\ M_{\odot}$, Burrows et al. 1997), we have expressed the detection limits for companions in terms of mass and projected physical separation in Figs. 7-13. For comparison, we also plot the positions of the companions to these stars that have been discovered through radial velocity measurements. A typical detection limit of those studies is represented by a velocity modulation of 10 m s^{-1} for 1 $M_{\odot}$. The actual detection limits for many of these stars are presented by Cumming, Marcy, & Butler (1999).

3. Discussion

We have obtained Keck near-IR AO images of 25 of the ~ 60 known extrasolar planetary systems. From these data, we have identified faint sources near four of the targets and have measured the detection limits for companions. Using the Keck and Gemini AO systems, we have also obtained AO images at an additional epoch of three of the four primaries exhibiting nearby faint objects. We now discuss the candidate companions individually, evaluate the achieved detection limits, and examine implications of these new constraints on substellar companions. For reference during this discussion, we list the 25 planetary systems in Table 1 along with the latest values of separation and M sin i for their radial velocity companions, upper limits to the masses of these companions from *Hipparcos* astrometry (Zucker & Mazeh 2001; see also Pourbaix & Arenou 2001), and recent age estimates.

Faint point sources have been detected in the Keck AO images of HD 37124, HD 168443, HD 187123, and HD 190228, which could be either companions or background field stars. These four star are all located at low galactic latitude ($|b| < 6°$), which suggests that most of the faint sources are background field stars rather than companions. For the star HD 168443 in particular, which is only 20° from the Galactic center and has $b = 2.^{\circ}5$, the presence of nine nearby objects at comparable magnitudes ($H \sim$ 17-19) is suggestive of a background star population. Because of the high proper motions of the targets in our sample and the high spatial resolution of AO imaging, multi-epoch observations spanning a year or less can easily distinguish companions from background stars. Such data were obtained for five of the 15 candidate companions, as listed in Table 2. All of these five objects exhibit proper motions relative to the primary stars that are consistent with those expected of background stars. Between 2000 September 18 and 2001 October 7, the position of the object near HD 37124 changed by ($\Delta\alpha$, $\Delta\delta$)=($0.''104$, $0.''388$)$\pm 0.''03$, which is close to the relative motion of ($0.''0839 \pm 0.''0014$, $0.''4418 \pm 0.''0009$) expected for a stationary background star given the *Hipparcos* proper motion of HD 37124. The two objects near HD 187123 were observed at two epochs by Keck. In data obtained at a third epoch by Gemini, the fainter source fell below the detection limit. The position of the brighter object changed by ($-0.''193$, $0.''157$)$\pm 0.''03$ relative to HD 187123 from 2000 June 27 to 2001 October 7, which is consistent with the motion of ($-0.''1831 \pm 0.''0007$, $0.''1577 \pm 0.''0008$) expected for a stationary background star. From 2000 June 27 to September 17, the offsets between the two candidate companions to HD 187123 are expected to have changed by $\sim 0.''03$ in right ascension and declination if one was a background star and the other was a companion. Since the sources remained fixed relative to each other at a level of $\lesssim 0.''005$, the fainter source also must be background star. Multi-epoch data were obtained for two of the sources near HD 168443. Between 2000 May 10 and September 17, the positions of two of the objects relative to HD 168443 changed by ($0.''078$, $0.''078$)$\pm 0.''03$ and ($0.''077$, $0.''085$)$\pm 0.''03$. These measurements are

consistent with the motion of background stars, which is expected to be ($\Delta\alpha$, $\Delta\delta$)=(0.″033, 0.″080) given the proper motion of HD 168443. Because of the low galactic latitude of HD 168443 and HD 190228 ($|b| < 3°$), the remaining faint sources detected near these two stars are probably background stars as well.

Rather than simply the discovery of low-mass companions, the primary objective of this study has been to obtain new, highly sensitive constraints on the presence of companions near a sample of planetary systems. These constraints are summarized and quantified by the point source detection limits in Figs. 7-13. From the plots of separation versus ΔH, we see that AO on the Keck II telescope produces high-contrast images in which point sources at $\Delta H = 10$ can be detected at 1″ from a bright star (see Figure 1). As a result, these data are sensitive to L and T dwarf companions to the targets at separations from 0.″5 (L0) to 2″ (Gl 570D). For comparison, the companion search towards field stars by Oppenheimer et al. (2001) probed 3-30″ and discovered the brown dwarf Gl 228B at a separation of 7.″8. In recent coronographic AO images of the planet-bearing star Gl 86, Els et al. (2001) identified a probable brown dwarf companion at 1.″72, $H = 14.4$, and $\Delta H = 10$. Gl 86 and ρ^1 55 Cnc have similar distances and brightnesses, and our detection limit for the latter indicates that the companion to Gl 86 would have been detected in our program as well. When these detection limits are transformed to units of companion mass and physical separation, they can be compared to the sensitivities of other methods of searching for substellar companions. The most fruitful of these techniques has been radial velocity monitoring, which currently reaches companions at $\lesssim 5$ AU that induce modulations of $\gtrsim 10$ m s^{-1}. As demonstrated in Figs. 7-13, our AO survey nicely complements the radial velocity work by probing for companions at wider separations, typically stars at 3-10 AU and brown dwarfs at 10-100 AU. The sensitivity to companions in direct imaging is improved with less massive and closer primary stars, which is illustrated by our data for the M dwarf Gl 876, where brown dwarfs are detectable at 1-10 AU.

Several stars in our sample deserve further comment given the new constraints on the presence of companions from this study. As already noted, the AO detection limits approach but do not reach the separations and masses of the substellar objects that have been inferred from radial velocity measurements to date. However, in a few cases, the AO data do place upper limits on the masses of those unseen companions. On the dates of our observations, radial velocity measurements predict minimum angular separations of 0.″04 and 0.″231 for the two companions to 47 UMa and 0.″148 for the companion to 14 Her (G. Marcy, private communication). While we cannot constrain the mass of the inner companion to 47 UMa, our non-detections correspond to a mass upper limit of 0.3 $M_\odot$ for each of the other two companions. The currently measured orbit for the putative companion to ϵ Eri is too uncertain to reliably predict the minimum angular separation, but our data do suggest that the companion is unlikely to be a star. As the time baselines of the radial velocity studies become longer, additional companions may be discovered at larger separations (see Table 1), and these AO data could be useful in constraining their masses as well. However, upper limits from *Hipparcos* are often much lower. Finally, Gonzales et al. (2001) found that HD 46375 and HD 37124 are overluminous on the Hertzsprung-Russell diagram by 0.5 and 0.25 mag at V, respectively. They suggest that these stars may have unresolved stellar companions that are beyond the maximum separations of 5 AU probed by radial velocity measurements. However, at projected separations of $> 0.″1$ (> 3.3 AU for each star), we find no companions that are sufficiently bright to account for the discrepancies in the luminosities. Other constraints on the presence of companions from the literature are noted in Table 1.

4. Conclusion

We have conducted a survey for companions to 25 of the ~ 60 known extrasolar planetary systems using near-IR AO imaging at Keck Observatory. The Keck II AO system has produced high-resolution images that approach the diffraction limit with a typical value of $0\farcs04$ for the FWHM in the H band. Using a variety of neutral density filters, exposure times, and position angles, we arrived at a set of images for each target that provides optimum sensitivity for all separations from $0\farcs1$ to $3\farcs3$.

After searching the AO images for candidate companions, near HD 37124, HD 168443, HD 187123, and HD 190228 we have identified 15 faint point sources (H = 14-20), all of which would be at or below the hydrogen burning mass limit if they were companions. Using AO imaging at Keck and Gemini Observatories, we have obtained images at a second epoch for five of the brightest candidate companions. These sources all exhibit proper motions relative to the central stars that are consistent with those expected of background stars. The remaining faint sources are probably background stars as well given the low galactic latitude of the four targets.

We have measured the point source detection limits for the AO images, which are presented in terms of both angular separation versus ΔH and projected physical separation versus companion mass. The sensitivities correspond to $\Delta H = 10$ at $1''$ and L and T dwarfs at $0\farcs5$ to $2''$ from the planet-bearing stars (H = 2-6). These data reach companion stars and brown dwarfs at 3-10 AU and 10-100 AU from the planet-bearing stars in this study, providing an essential complement to previous radial velocity measurements of these systems ($> 0.3\ M_{\rm Jup}$, < 5 AU).

We wish to thank Peter Wizinowich, Scott Acton, David Le Mignant and the rest of the Keck Observatory staff for their support. We also thank Kathy Roth, Francois Rigaut, Mark Chun, Olivier Guyon, and Dan Potter for their assistance in obtaining the observations at Gemini Observatory. We are grateful to Joan Najita for help with an earlier Keck proposal, and to Geoff Marcy for calculating the positions of the radial velocity companions to 47 UMa and 14 Her. We thank Geoff Marcy, Debra Fischer, and Jamie Lloyd for useful discussions. K. L. was supported by a postdoctoral fellowship at the Harvard-Smithsonian Center for Astrophysics. R. J. was supported by a Miller Research Fellowship. This work was supported in part by the Smithsonian Institution, NASA, and NSF grants to Geoff Marcy, and a NASA grant to R.J. administered by the AAS. This publication makes use of data products from the Two Micron All Sky Survey, which is a joint project of the University of Massachusetts and the Infrared Processing and Analysis Center, funded by the National Aeronautics and Space Administration and the National Science Foundation. Some of the data presented herein were obtained at the W. M. Keck Observatory, which is operated as a scientific partnership among the California Institute of Technology, the University of California, and the National Aeronautics and Space Administration. The Observatory was made possible by the generous financial support of the W. M. Keck Foundation. We wish to extend special thanks to those of Hawaiian ancestry on whose sacred mountain we are privileged to be guests. Without their generous hospitality, some of the observations presented herein would not have been possible. Some of these observations were obtained at the Gemini Observatory, which is operated by the Association of Universities for Research in Astronomy, Inc., under a cooperative agreement with the NSF on behalf of the Gemini partnership: the National Science Foundation (United States), the Particle Physics and Astronomy Research Council (United Kingdom), the National Research Council (Canada), CONICYT (Chile), the Australian Research Council (Australia), CNPq (Brazil) and CONICET (Argentina). This paper includes data obtained with the Adaptive Optics System Hokupa'a/Quirc, developed and operated by the University of Hawaii Adaptive Optics Group, with support from the National Science Foundation. Finally, we thank the anonymous referee for useful comments

that improved this manuscript.

REFERENCES

Allard, F., Hauschildt, P. H., Baraffe, I., & Chabrier, G. 1996, ApJ, 465, L123

Baraffe, I., Chabrier, G., Allard, F., & Hauschildt, P. H. 1998, A&A, 337, 403

Bessell, M. S. 1991, AJ, 101, 662

Brown, T. M., Charbonneau, D., Gilliland, R. L., Noyes, R. W., & Burrows, A. 2001, ApJ, 552, 699

Burrows, A., et al. 1997, ApJ, 491, 856

Butler, R. P., et al. 1999, ApJ, 526, 916

Butler, R. P., Marcy, G. W., Vogt, S. S., & Apps, K. 1998, PASP, 110, 1389

Butler, R. P., Marcy, G. W., Williams, E., Hauser, H., & Shirts, P. 1997, ApJ, 474, L115

Butler, R. P., Vogt, S. S., Marcy, G. W., Fischer, D. A., Henry, G. W., & Apps, K. 2000, ApJ, 545, 504

Charbonneau, D., Brown, T. M., Latham, D. W., & Mayor, M. 2000, ApJ, 529, L45

Close, L. M., Potter, D., Brandner, W., Lloyd-Hart, M., Liebert, J., Burrows, A., & Siegler, N. 2002, ApJ, in press

Cochran, W. D., Hatzes, A. P., Butler, R. P., & Marcy, G. W. 1997, ApJ, 483, 457

Cumming, A., Marcy, G. W., & Butler, R. P. 1999, ApJ, 526, 890

Delfosse, X., Forveille, T., Beuzit, J.-L., Udry, S., Mayor, M., & Perrier, C. 1999, A&A, 344, 897

Delfosse, X., Forveille, T., Mayor, M., Perrier, C., Naef, D., & Queloz, D. 1998, A&A, 338, 67

Els, S.G., Sterzik, M.F., Marchis, F., Pantin, E., Endl, M., & Kürster, M. 2001, A&A, 370, L1

Fischer, D. A., Marcy, G. W., Butler, R. P., Laughlin, G., & Vogt, S. S. 2001a, ApJ, in press

Fischer, D. A., Marcy, G. W., Butler, R. P., Vogt, S. S., & Apps, K. 1999, PASP, 111, 50

Fischer, D. A., Marcy, G. W., Butler, R. P., Vogt, S. S., Frink, S., Apps, K. 2001b, ApJ, 551, 1107

Ford, E. B., Rasio, F. A., & Sills, A. 1999, ApJ, 514, 411

Fuhrmann, K., Pfeiffer, M. J., & Bernkopf, J. 1997, A&A, 326, 1081

Fuhrmann, K., Pfeiffer, M. J., & Bernkopf, J. 1998, A&A, 336, 942

Gizis, J. E., Kirkpatrick, J. D., Burgasser, A., Reid, I. N., Monet, D. G., Liebert, J., & Wilson, J. C. 2001, ApJ, 551, L163

Gonzalez, G. 1998, A&A, 334, 221

Gonzalez, G. 1999, MNRAS, 308,, 447

Gonzalez, G., & Laws, C. 2000, AJ, 119, 390

Gonzalez, G., Laws, C., Tyagi, S., & Reddy, B. 2001, AJ, 121, 432

Gonzalez, G., & Vanture, A. D. 1998, ApJ, 339, 29

Graves, J. E., Northcott, M. J., Roddier, F. J., Roddier, C. A., & Close, L. M. 1998, Proc. S.P.I.E., 3353, 34

Greaves, J. S., et al. 1998, ApJ, 506, 133

Hatzes, A. P., et al. 2000, ApJ, 544, L145

Henry, G. W., Baliunas, S. L., Donahue, R. A., Fekel, F. C., & Soon, W. H. 2000a, ApJ, 531, 415

Henry, G. W., Marcy, G. W., Butler, R. P., & Vogt, S. S. 2000b, ApJ, 529, L41

Kenyon, S. J., & Hartmann, L. 1995, ApJS, 101, 117

Kirkpatrick, J. D., et al. 2000, AJ, 120, 447

Lachaume, R., Dominik, C., Lanz, T., & Habing, H. J. 1999, A&A, 348, 897

Leggett, S. K., Allard, F., Berriman, G., Dahn, C. C., & Hauschildt, P. H. 1996, ApJS, 104, 117

Leggett, S. K., Allard, F., Geballe, T. R., Hauschildt, P. H., & Schweitzer, A. 2001, ApJ, 548, 908

Leggett, S. K., Toomey, D. W., Geballe, T. R., & Brown, T. R. 1999, ApJ, 517, L139

Luhman, K. L. 1999, ApJ, 525, 466

Marcy, G. W., & Butler, R. P. 1996, ApJ, 464, L153

Marcy, G. W., & Butler, R. P. 1998, ARA&A, 36, 57

Marcy, G. W., Butler, R. P., Vogt, S. S., Fischer, D., & Lissauer, J. J. 1998, ApJ, 505, L147

Marcy, G. W., Butler, R. P., Vogt, S. S., Fischer, D., & Liu, M. 1999, ApJ, 520, 239

Marcy, G. W., Butler, R. P., & Vogt, S. S. 2000a, ApJ, 536, L43

Marcy, G. W., Cochran, W. D., & Mayor, M. 2000b, in *Protostars and Planets IV*, ed. V. Mannings, A.P. Boss, S.S. Russell (Tucson: University of Arizona Press), 1285

Marcy, G. W., Butler, R. P., Fischer, D. A., Vogt, S. S., Lissauer, J. J., & Rivera, E. J. 2001a, ApJ, 556, 296

Marcy, G. W., Butler, R. P., Vogt, S. S., Liu, M. C., Laughlin, G., Apps, K., Graham, J. R., Lloyd, J., Luhman, K. L., & Jayawardhana, R. 2001b, ApJ, 555, 418

Marley, M. S., Saumon, D., Guillot, T., Freedman, R. S., Hubbard, W. B., Burrows, A., & Lunine, J. I. 1996, Science, 272, 1919

Martín, E. L., Koresko, C. D., Kulkarni, S. R., Lane, B. F., & Wizinowich, P. L. 2000, ApJ, 529, L37

Mazeh, T., et al. 2000, ApJ, 532, L55

Mayor, M., & Queloz, D. 1995, Nature, 378, 355

Monet, D. G., Dahn, C. C., Vrba, F. J., Harris H. C., Pier, J. R., Luginbuhi, C. B., & Ables, H. D. 1992, AJ, 103, 638

Naef, D., Mayor, M., Pepe, F., Queloz, D., Santos, N. C., Udry, S., & Burnet, M. 2001, A&A, 375, 205

Nakajima, T., Oppenheimer, B. R., Kulkarni, S. R., Golimowski, D. A ., Matthews, K., & Durrance, S. T. 1995, Nature, 378, 463

Ng, Y. K., & Bertelli, G. 1998, A&A, 329, 943

Noyes, R. W., et al. 1997, ApJ, 483, L111

Oppenheimer, B. R., Golimowski, D. A., Kulkarni, S. R., Matthews, K., Nakajima, T., Creech-Eakman, M., & Durrance, S. T. 2001, AJ, 121, 2189

Pourbaix, D., & Arenou, F. 2001, A&A, 372, 935

Queloz, D., Mayor, M., Naef, D., Pepe, F., Santos, N.C., Udry, S., & Burnet, M. 2001, in Planetary Systems in the Universe: Observation, Formation and Evolution, IAU Symp. 202, Eds. A. Penny, P. Artymowicz, A.-M. Lagrange and S. Russel ASP Conf. Ser., in press

Reid, I. N., Burgasser, A. J., Cruz, K. L., Kirkpatrick, J. D., & Gizis, J. E. 2001a, AJ, 121, 1710

Reid, I. N., Gizis, J. E., Kirkpatrick, J. D., & Koerner, D. W. 2001b, AJ, 121, 1710

Rivera, E. J., & Lissauer, J. J. 2000, ApJ, 530, 454

Schmidt-Kaler, T. 1982, in Landolt-Bornstein, Group VI, Vol. 2, ed. K.-H. Hellwege (Berlin: Springer), 454

Schroeder, D. J., et al. 2000, AJ, 119, 906

Schweitzer, A., Gizis, J. E., Hauschildt, P. H., Allard, F., Howard, E. M., & Kirkpatrick, J. D. 2001, ApJ, in press

Sivan, J.-P., Mayor, M., Naef, D., Queloz, D., Udry, S., Perrier-Bellet, C., & Beuzit, J. 2001, in Planetary Systems in the Universe: Observation, Formation and Evolution, IAU Symp. 202, Eds. A. Penny, P. Artymowicz, A.-M. Lagrange and S. Russel ASP Conf. Ser., in press

Smith, V. V., Cunha, K., & Lazzaro, D. 2001, AJ, 121, 3207

Song, I., Caillault, J.-P., Barrado y Navascúes, D., Stauffer, J. R., & Randich, S. 2000, ApJ, 533, 41

Tinney, C. G., et al. 2001, ApJ, 551, 507

Tinney, C. G., Mould, J. R., & Reid, I. N. 1993, AJ, 105, 1045

Udry, S., Mayor, M., & Queloz, D., 2001, in Planetary Systems in the Universe: Observation, Formation and Evolution, IAU Symp. 202, Eds. A. Penny, P. Artymowicz, A.-M. Lagrange and S. Russel ASP Conf. Ser., in press

Vogt, S. S., Marcy, G. W., Butler, R. P., & Apps, K. 2000, ApJ, 536, 902

Wizinowich, P., et al. 2000, PASP, 112, 315

Zucker, S., & Mazeh, T. 2001, ApJ, in press

This preprint was prepared with the AAS LaTeX macros v5.0.

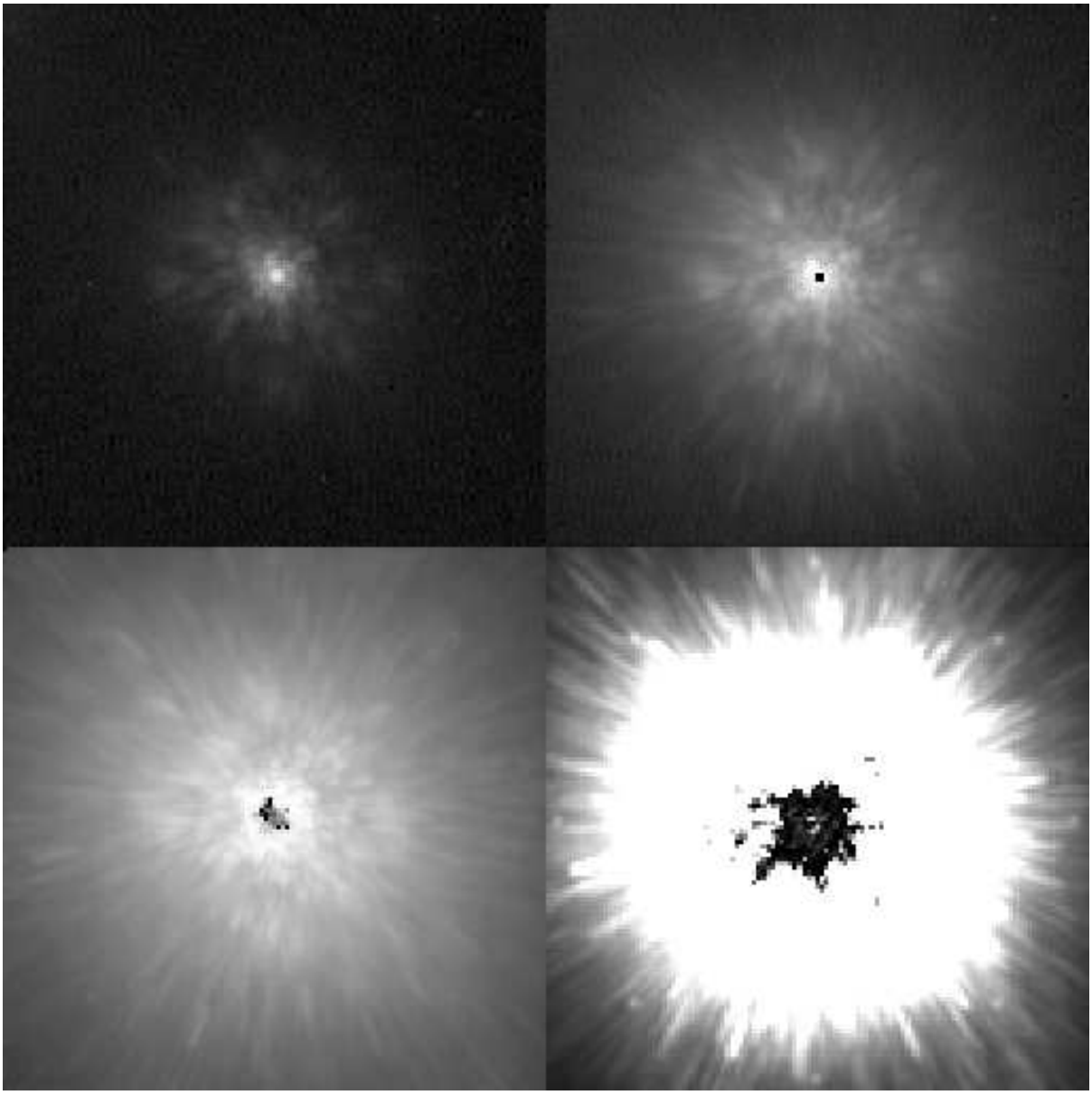

Fig. 1.— Keck AO images of 51 Peg ($2\farcs11 \times 2\farcs11$) through the H-band filter and the N3, N2, N1, and open filters (upper left through lower right). The displays of the first three images are scaled logarithmically from zero counts to the saturation level. In the image with the open filter, eight artificial stars have been inserted at intervals of 45° surrounding the primary to illustrate the point source detection limit of $\Delta H = 10$ at $1''$. The display is scaled linearly across a range that is optimized for viewing the artificial stars. Each image is the average of six 2 sec exposures.

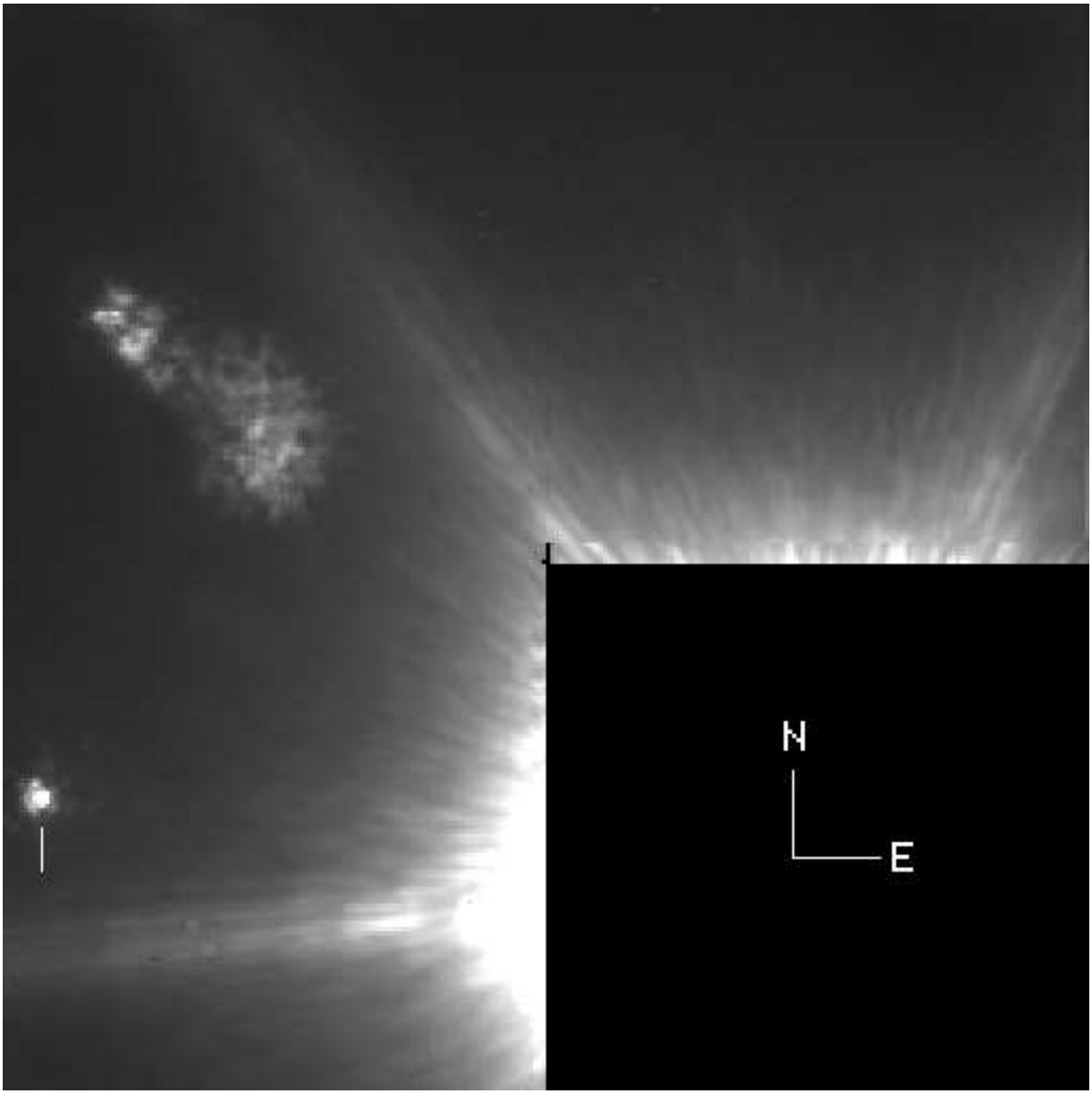

Fig. 2.— A Keck AO image towards HD 37124 ($4\farcs36 \times 4\farcs36$) through the H-band filter. A point source is detected in the lower left quadrant of the image ($H = 14.9$). The proper motion of this source relative to HD 37124 is indicative of a background star. The image is the average of six 30 sec exposures and is displayed with a linear scale. A ghost image from HD 37124 appears in the upper left quadrant.

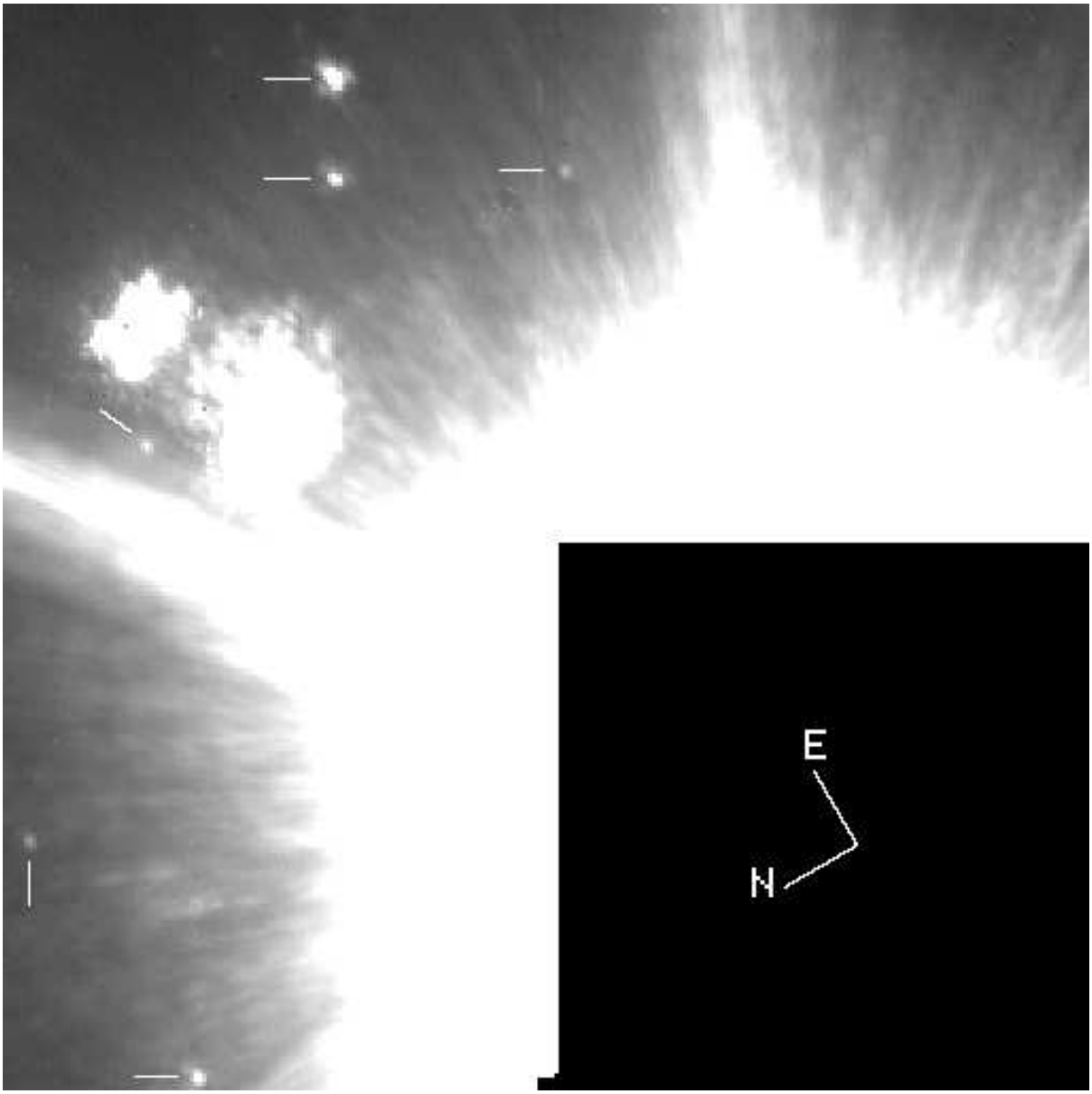

Fig. 3.— A Keck AO image towards HD 168443 ($4\farcs36 \times 4\farcs36$) through the H-band filter. Six point sources are detected in this image ($H = 16.4$-19). The ghost image from HD 168443 in the upper left quadrant falls on top of a seventh point source that is detected in other images of this star. Proper motions relative to HD 168443 are available for only the two brightest objects; those measurements are indicative of background stars. The image is the average of six 30 sec exposures. The display is scaled linearly across a range that is optimized for viewing the six point sources.

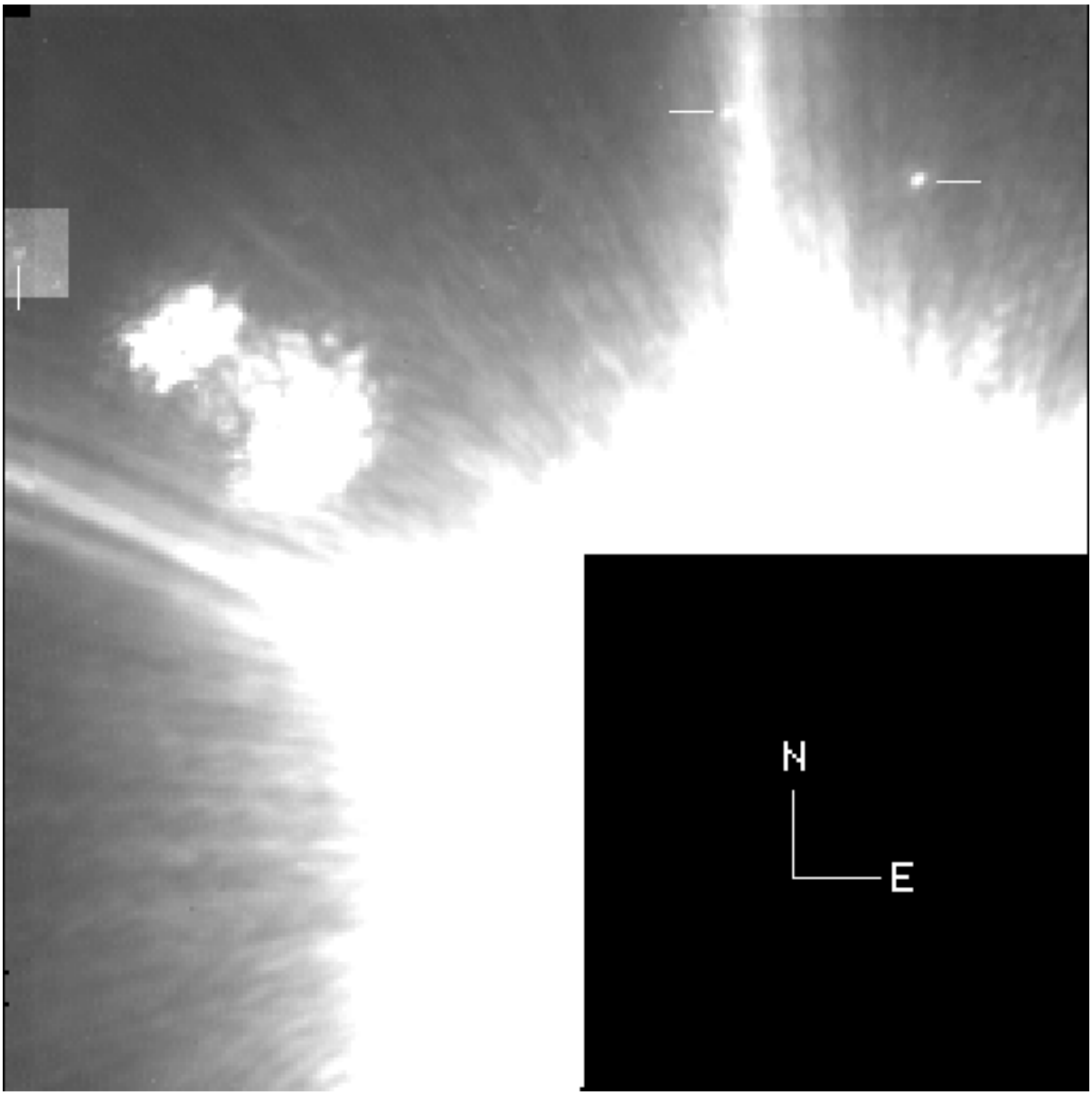

Fig. 4.— A Keck AO image towards HD 168443 ($4\farcs36 \times 4\farcs36$) through the H-band filter. Three point sources are detected in the image (H = 17.6-19). The image is the average of six 30 sec exposures. The display is scaled linearly across a range that is optimized for viewing the three point sources, where a separate scaling is used for the area surrounding the faintest object at the far left. A ghost image from HD 168443 appears in the upper left quadrant.

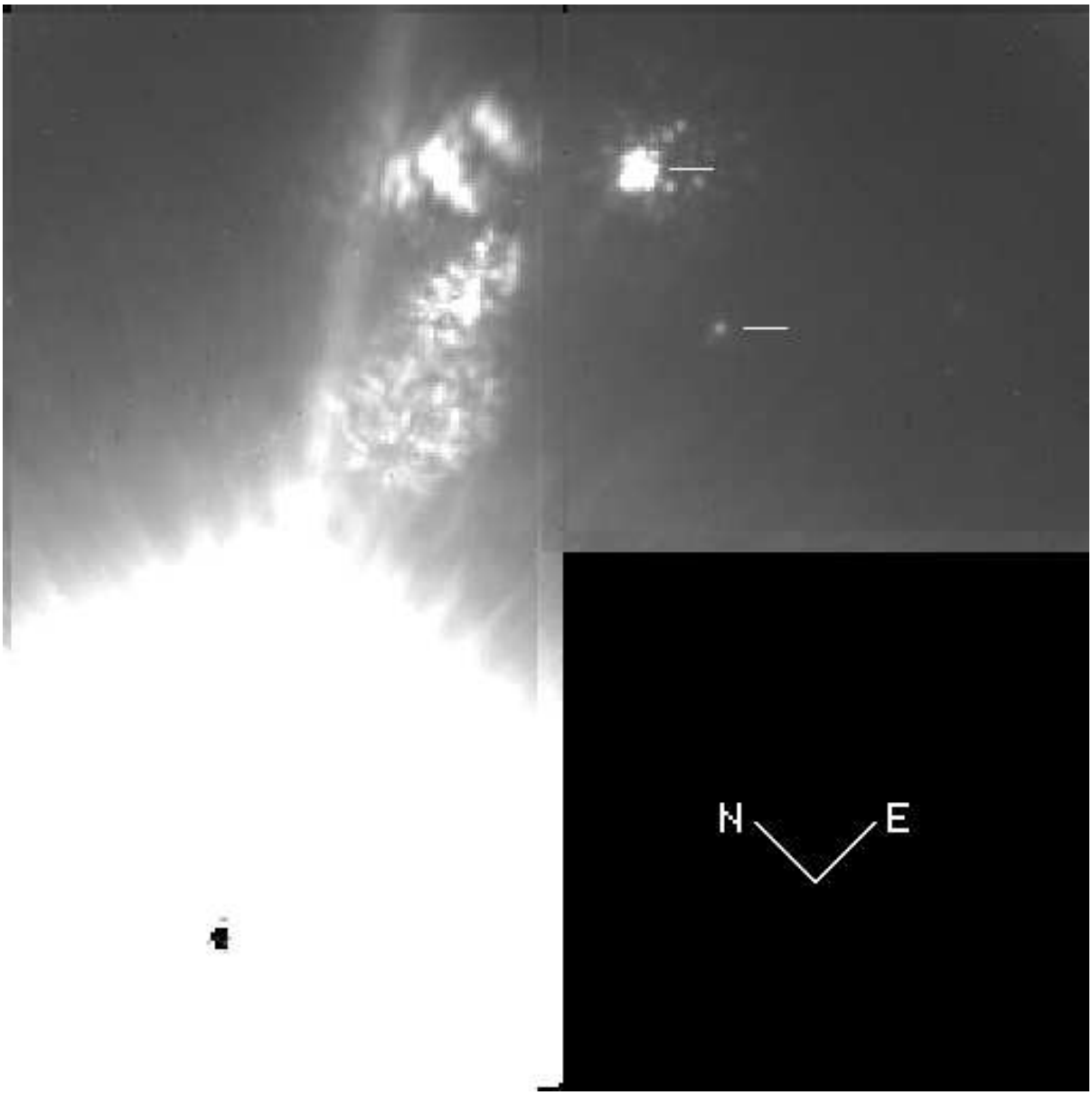

Fig. 5.— A Keck AO image towards HD 187123 (4.″36 × 4.″36). Two point sources are detected in the upper right quadrant (H = 14.2 and 18.3). The proper motions of these sources relative to HD 187123 are indicative of background stars. The image is the average of six 30 sec exposures. The display is scaled linearly across a range that is optimized for viewing the two point sources. A ghost image from HD 187123 appears in the upper left quadrant.

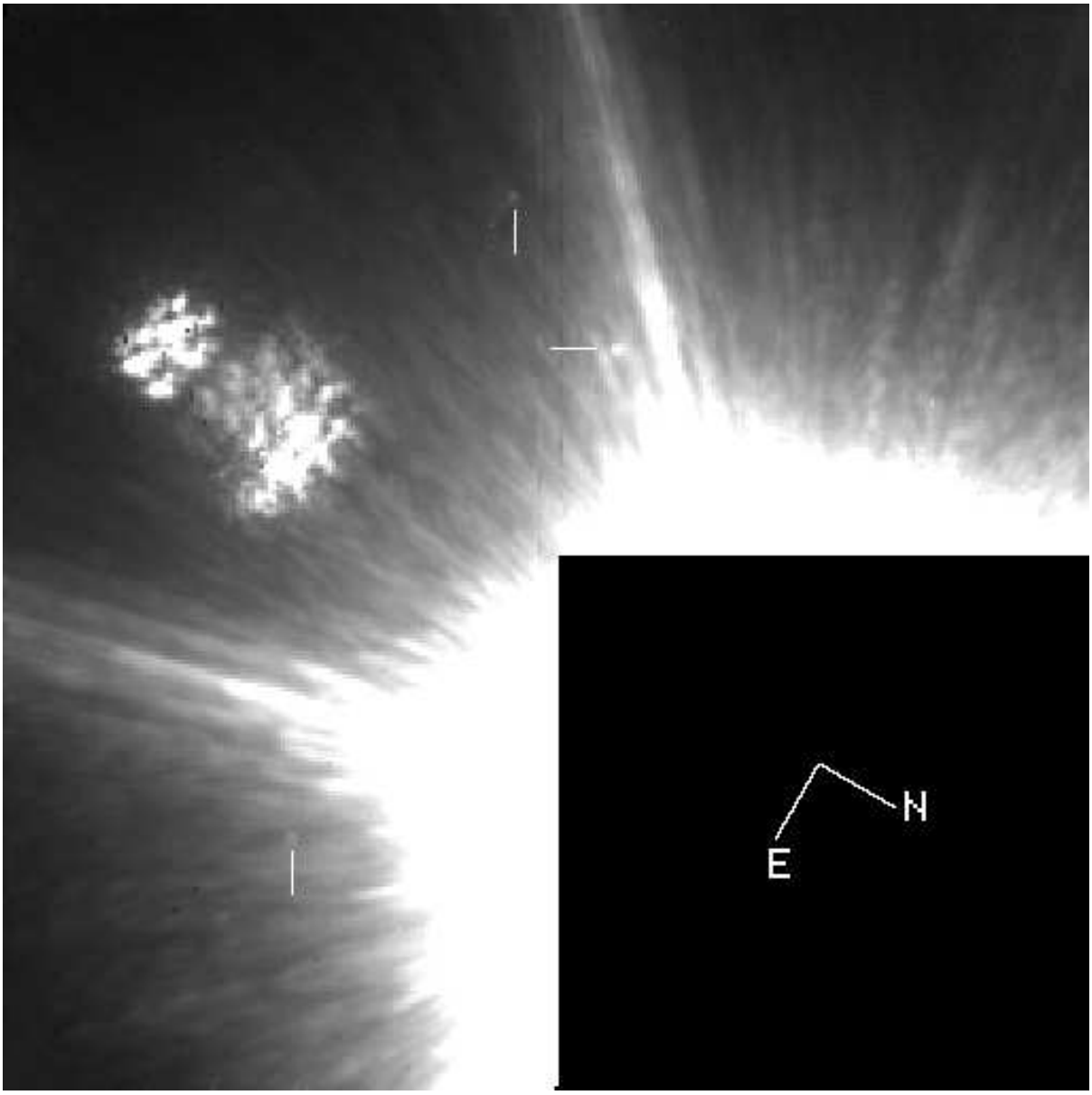

Fig. 6.— A Keck AO image towards HD 190228 ($4\farcs36 \times 4\farcs36$). Three point sources are detected in the image ($H = 18.5$-19). The image is the average of six 30 sec exposures. The display is scaled linearly across a range that is optimized for viewing the three point sources. A ghost image from HD 190228 appears in the upper left quadrant.

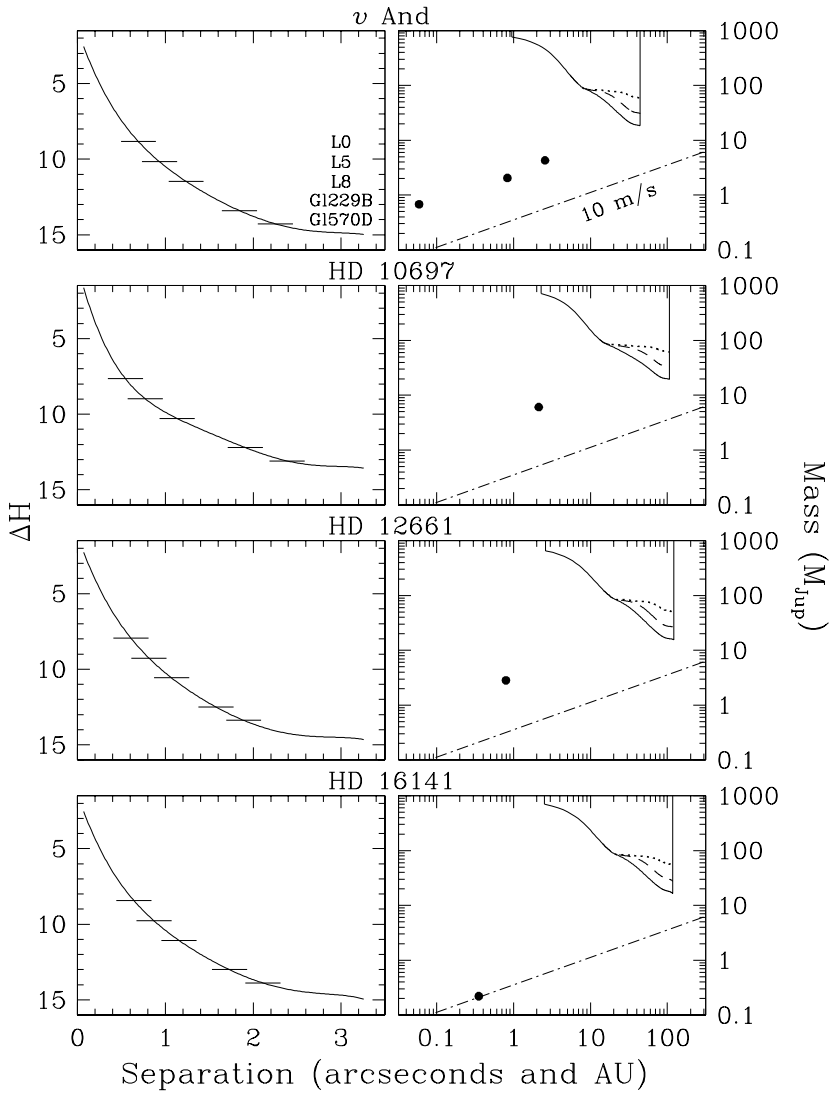

Fig. 7.— *Left:* The solid curves represent the 6 σ detection limits for point sources in Keck AO images of υ And, HD 10697, HD 12661, and HD 16141 as a function of angular separation and after subtracting the H-band magnitude of each star. The short horizontal lines along the detection limits indicate the magnitudes of typical L0, L5, and L8 field dwarfs and the T dwarfs Gl 229B and Gl 570D placed at the distances of these stars (Kirkpatrick et al. 2000). *Right:* The measured detection limits from the left are plotted in terms of mass and projected physical separation assuming ages of 1 (*solid*), 3 (*dashed*), and 10 Gyr (*dotted*) (Burrows et al. 1997; Baraffe et al. 1998). The solid points represent the values of M sin i and the semi-major axis of companions to these stars as measured in radial velocity studies. Recent stellar age estimates and additional constraints on the companion masses are found in Table 1. A velocity modulation of 10 m s^{-1} for a solar-mass central star is shown as the dot-dashed line.

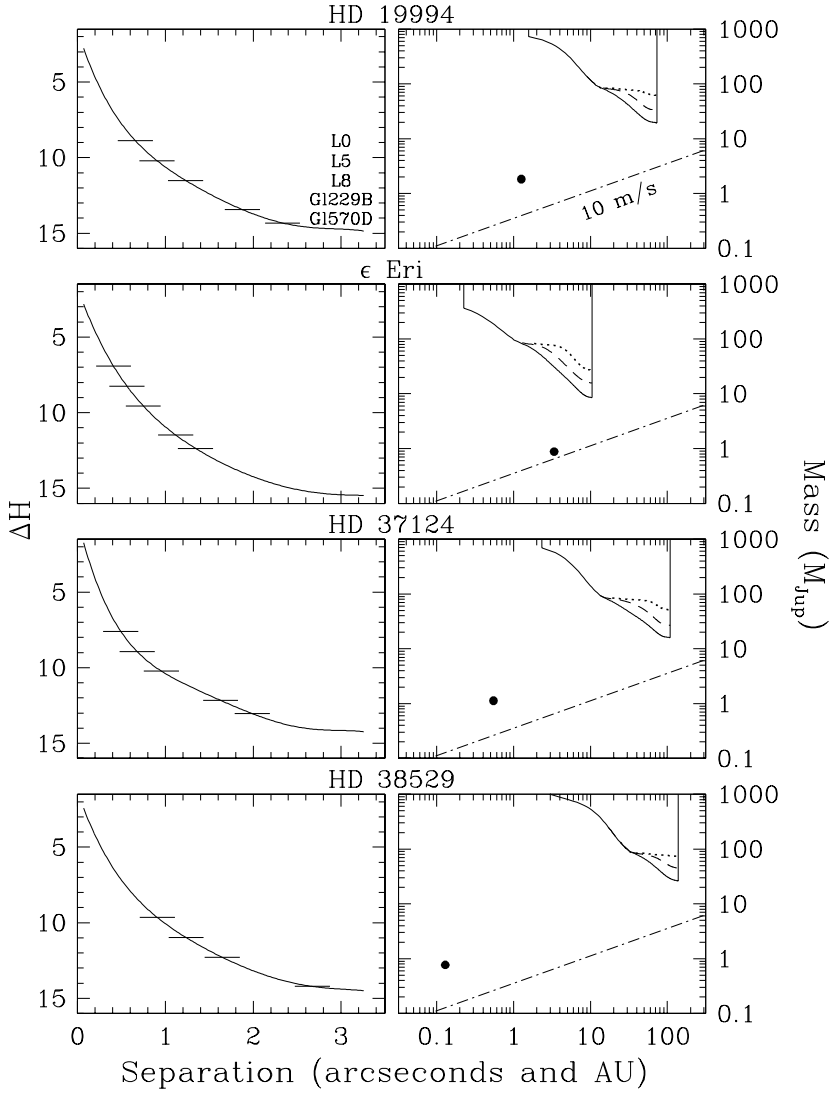

Fig. 8.— Same as Figure 7, but for HD 19994, ϵ Eri, HD 37124, and HD 38529. Gl 570D would not be detected in the data for HD 38529.

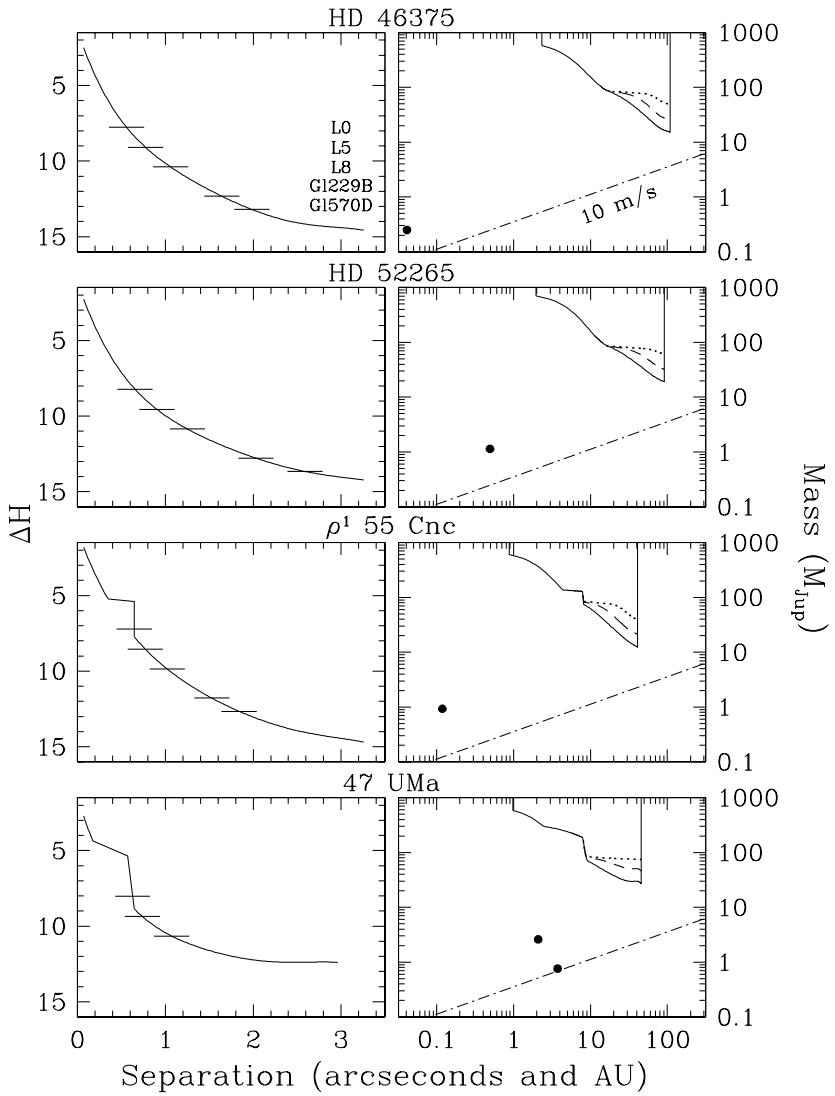

Fig. 9.— Same as Figure 7, but for HD 46375, HD 52265, ρ^1 55 Cnc, and 47 UMa. In the data for 47 UMa, Gl 229B would fall at the detection limit at separations beyond 2″ and Gl 570D would not be detected.

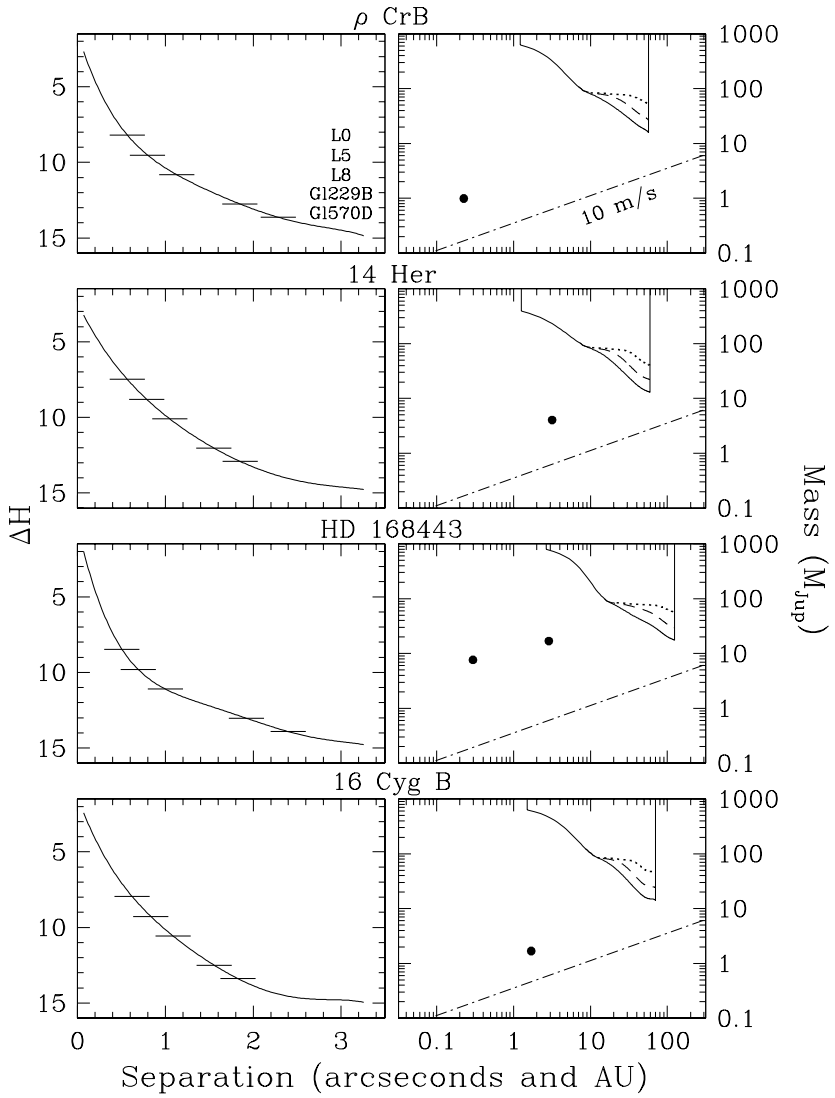

Fig. 10.— Same as Figure 7, but for ρ CrB, 14 Her, HD 168443, and 16 Cyg B.

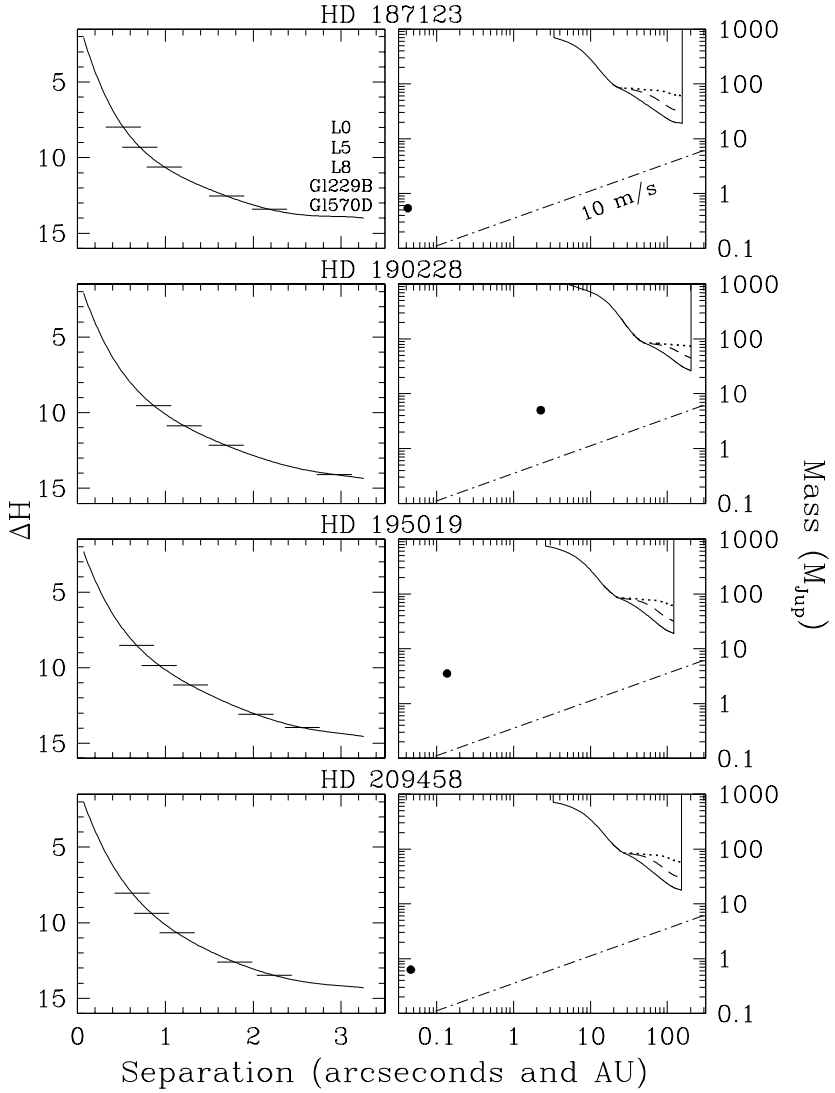

Fig. 11.— Same as Figure 7, but for HD 187123, HD 190228, HD 195019, and HD 209458. Gl 570D would not be detected in the data for HD 190228.

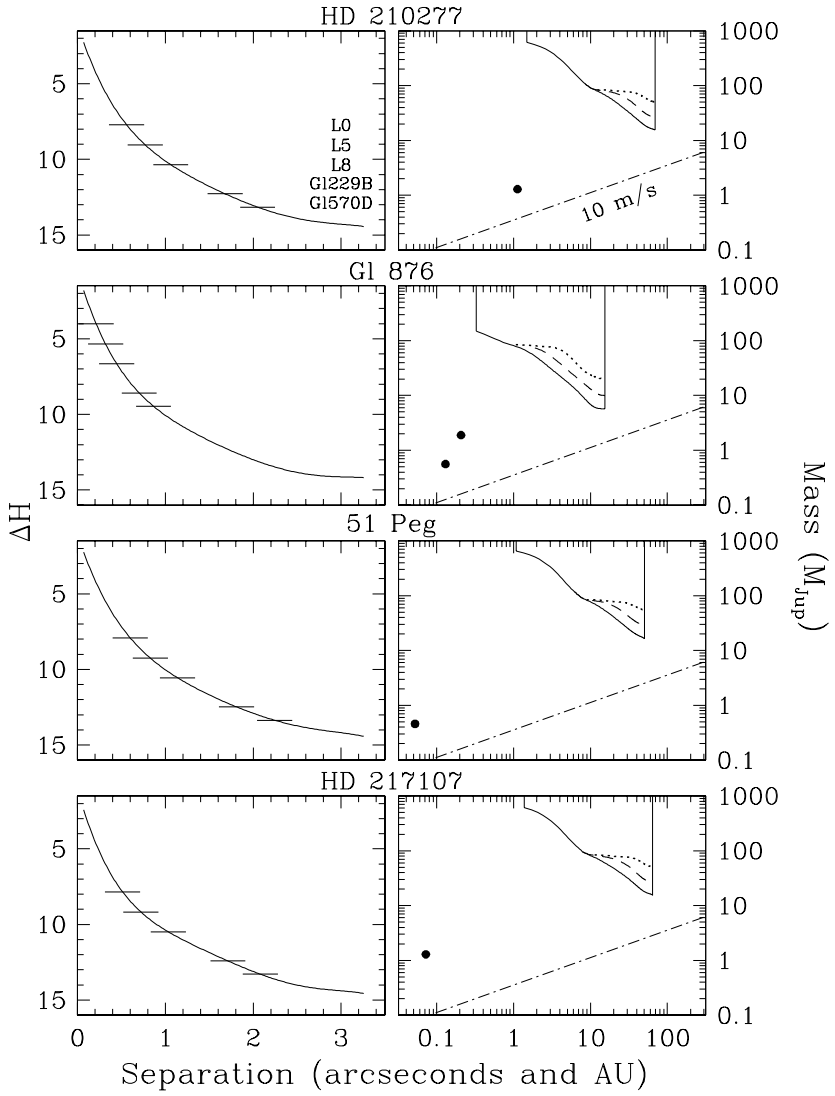

Fig. 12.— Same as Figure 7, but for HD 210277, Gl 876, 51 Peg, and HD 217107.

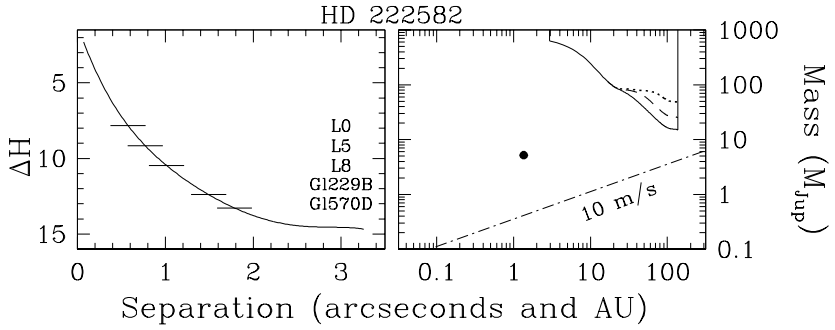

Fig. 13.— Same as Figure 7, but for HD 222582.

Table 1. Properties of Planetary Systems

Star	a[a] (AU)	$M \sin i$[a] ($M_{\rm Jup}$)	References	M_{Hip}[b] ($M_{\rm Jup}$)	Stellar Age (Gyr)	References
υ And	0.059	0.58	1	···	3.8 ± 1, 2.7 ± 0.3, $2.6^{+2.1}_{-1}$, 2.9 ± 0.6, 3.3 ± 0.5, < 4	2, 3, 4, 5, 6, 7
	0.828	2.05	8, 9	···		
	2.56	4.29	8, 9	< 19		
HD 10697	2.12	6.08	10	< 92	7.8 ± 0.5, 6.0	11
HD 12661	0.795	2.84	12	< 140	8 ± 1, 8.4	11
HD 16141	0.351	0.22	13	< 530	8.5 ± 0.5, 6.7	11
HD 19994	1.26	1.83	14	< 66	3 ± 0.3, 4.3	3, 15
ϵ Eri[c]	3.36	0.88	16	< 22	0.5-1, 0.73 ± 0.2	17, 18
HD 37124	0.547	1.13	10	< 480	3.9	11
HD 38529[d]	0.129	0.77	9	···	3 ± 0.5, 3.7	11
HD 46375	0.041	0.25	13	···	4.5	11
HD 52265	0.493	1.14	12, 19	< 140	2.1 ± 0.3, 4.0, 3.5	8, 8, 19
ρ^1 55 Cnc[e]	0.118	0.93	1	< 290	< 5, 4 ± 3, 5, $8.4^{+7.1}_{-8.3}$, 4-5	2, 20, 21, 4, 7
47 UMa	2.09	2.54	22	< 15	7.3 ± 1.9, $6.6^{+1.5}_{-1.3}$, 8 ± 2, 6.3, $6.3^{+2}_{-2.4}$, 6	23, 3, 24, 21, 5, 7
	3.73	0.76	25	···		
ρ CrB	0.224	0.99	26	< 230	10.2 ± 1.7, 12.1 ± 1.1, 11 ± 2, 12.3, $14.1^{+2}_{-2.4}$, 6	2, 3, 24, 21, 4, 7
14 Her	3.17	4.05	27	< 20	6	28, 21
HD 168443	0.295	7.64	29	···	10.5 ± 1.5, 7.4, 8	11, 11, 30
	2.87	16.96	30, 31	< 80		
16 Cyg B	1.69	1.68	32	< 27	8 ± 1.8, 9 ± 2, 9, 6-7	2, 24, 21, 7
HD 187123[f]	0.042	0.54	33	···	$4^{+1}_{-0.5}$, 5.5	28, 21
HD 190228	2.25	5.01	34	< 77	···	···
HD 195019	0.136	3.55	35	< 1470	3	35
HD 209458	0.046	0.63[g]	36, 37	···	4.5, 3 ± 1, 4.3	38, 11, 11
HD 210277[h]	1.12	1.29	29, 19	< 40	12 ± 2, 8.5	28, 21
Gl 876	0.207	1.89	39, 40	< 51	1-10	39
	0.130	0.56	41	···		
51 Peg	0.052	0.46	42	< 1080	4 ± 2.5, $7.0^{+1.1}_{-0.9}$, $7.6^{+4}_{-5.1}$, $5.1^{+3}_{-0.7}$, 7, 5.5 ± 0.5, 7.1	23, 3, 4, 5, 7, 11, 11
HD 217107[i]	0.072	1.29	35	< 1670	8, 12 ± 1.5, 5.6	35, 11, 11
HD 222582	1.35	5.18	10	< 150	11 ± 1, 5.6	11

[a] http://exoplanets.org.

[b] Constraints on companion masses derived from *Hipparcos* data and radial velocity measurements (Zucker & Mazeh 2001).

[c] Companion has a probable mass of ~ 1.7 $M_{\rm Jup}$ (Hatzes et al. 2000).

[d] May have an additional companion (Fischer et al. 2001b).

[e] May have an additional companion at ~ 5.5 AU and ~ 3.2 $M_{\rm Jup}$ (Butler et al. 1997; Fischer et al. 2001b).

[f] May have an additional companion (Vogt et al. 2000).

[g] $i = 86.^{\circ}6 \pm 0.^{\circ}14$ (Brown et al. 2001).

[h] No stellar companions at < 10 AU and 17-250 AU (Marcy et al. 1999, references therein).

[i] Companion has a probable mass upper limit of ~ 11 $M_{\rm Jup}$ (Fischer et al. 1999). May have an additional companion beyond a few AU and more massive than ~ 3 $M_{\rm Jup}$ (Vogt et al. 2000; Fischer et al. 2001b).

References. — (1) Butler et al. 1997; (2) Fuhrmann et al. 1998; (3) Ng & Bertelli 1998; (4) Ford et al. 1999; (5) Lachaume et al. 1999; (6) Gonzales & Laws 2000; (7) Henry et al. 2000a; (8) Butler et al. 1999; (9) Fischer et al. 2001b; (10) Vogt et al. 2000; (11) Gonzales et al. 2001; (12) Butler et al. 2000; (13) Marcy, Butler, & Vogt 2000a; (14) Queloz et al. 2001; (15) Smith, Cunha, & Lazzaro 2001; (16) Hatzes et al. 2000; (17) Greaves et al. 1998; (18) Song et al. 2000; (19) Naef et al. 2001; (20) Gonzalez & Vanture 1998; (21) Gonzalez 1999; (22) Marcy & Butler 1996; (23) Fuhrmann, Pfeiffer, & Bernkopf 1997; (24) Gonzalez 1998; (25) Fischer et al. 2001a; (26) Noyes et al. 1997; (27) Marcy et al. 2000b; (28) Gonzalez et al. 1999; (29) Marcy et al. 1999; (30) Marcy et al. 2001b; (31) Udry, Mayor, & Queloz 2001; (32) Cochran et al. 1997; (33) Butler et al. 1998; (34) Sivan et al. 2001; (35) Fischer et al. 1999; (36) Charbonneau et al. 2000; (37) Henry et al. 2000b; (38) Mazeh et al. 2000; (39) Marcy et al. 1998; (40) Delfosse et al. 1998; (41) Marcy et al. 2001a; (42) Mayor & Queloz 1995.

Table 2. Faint Sources Detected Near Planetary Systems

Star	$\Delta\alpha$[a] (arcsec)	$\Delta\delta$[a] (arcsec)	H (mag)	ΔH[b] (mag)	Obs Date
HD 37124	−3.076, −2.972	0.314, 0.702	14.9	8.9	9/18/00, 10/07/01
HD 168443	2.802	−0.413	18.5	13.1	9/17/00
	3.516, 3.594	0.129, 0.207	16.4	11.0	5/10/00, 9/17/00
	3.166, 3.243	0.318, 0.403	17.7	12.3	5/10/00, 9/17/00
	2.691	1.585	18.8	13.4	9/17/00
	1.554	2.789	19.0	13.6	9/17/00
	0.402	2.677	17.6	12.2	9/17/00
	−0.364	2.949	18.6	13.2	9/17/00
	−3.215	2.380	19.0	13.6	9/17/00
	2.973	1.502	~ 20	~ 14.6	9/17/00
HD 187123	3.364,3.361,3.171	0.973,0.994,1.130	14.2	7.8	6/27/00, 9/16/00, 10/07/01
	3.142,3.137	0.286,0.310	18.3	11.9	6/27/00, 9/16/00
HD 190228	0.999	−1.796	~ 19	~ 13.6	9/18/00
	−1.343	−1.644	~ 18.5	~ 13.1	9/18/00
	−1.664	−2.312	~ 19	~ 13.6	9/18/00

[a]Positions in right ascension and declination are measured with respect to the star. For a given star, the uncertainties in the positions of the faint sources relative to the star and relative to each other are $\pm 0\farcs02$ and $\pm 0\farcs004$, respectively. An exception is HD 190228, where the uncertainty in the former value is $\pm 0\farcs04$.

[b]Magnitude difference of the primary star and faint source.